Fundamental Noise Limitations to Supercontinuum Generation in Microstructure Fiber

K. L. Corwin,[1] N. R. Newbury,[1] J. M. Dudley,[2] S. Coen,[3] S. A. Diddams,[1] K. Weber,[1] and R. S. Windeler[4]

[1]*National Institute of Standards and Technology, 325 Broadway, Boulder, Colorado 80305*

[2]*Laboratoire d'Optique P. M. Duffieux, Université de Franche-Comté, 25030 Besançon, France*

[3]*Service d'Optique et Acoustique, Université Libre de Bruxelles, Avenue F. D. Roosevelt 50, CP 194/5, B-1050 Brussels, Belgium*

[4]*OFS Laboratories, 700 Mountain Avenue, Murray Hill, New Jersey 07974*

(Received 26 November 2002; published 21 March 2003)

Broadband noise on supercontinuum spectra generated in microstructure fiber is shown to lead to amplitude fluctuations as large as 50% for certain input laser pulse parameters. We study this noise using both experimental measurements and numerical simulations with a generalized stochastic nonlinear Schrödinger equation, finding good quantitative agreement over a range of input-pulse energies and chirp values. This noise is shown to arise from nonlinear amplification of two quantum noise inputs: the input-pulse shot noise and the spontaneous Raman scattering down the fiber.

DOI: 10.1103/PhysRevLett.90.113904 PACS numbers: 42.81.Dp, 02.60.Cb, 42.50.Lc, 42.65.Re

The generation of broadband supercontinuum spectra from the injection of femtosecond pulses into microstructure or tapered fibers has now been achieved by several groups [1,2]. The supercontinuum is a remarkable light source, exhibiting both spatial and phase coherence, while simultaneously spanning the entire visible spectrum with brightness exceeding that of a light bulb by at least 5 orders of magnitude. These unique properties should make the supercontinuum an ideal tool for important applications including optical coherence tomography [3] and spectroscopy [4,5]. Indeed, it has already led a revolution in frequency metrology, allowing the creation of optical atomic clocks with stability that exceeds the performance of the world's best microwave-based atomic clocks [5–7]. However, a significant broadband amplitude noise on the supercontinuum has been observed to limit its stability, interfering with optical clocks [8,9] and rendering the supercontinuum too noisy for many applications. This noise extends well beyond the frequency roll-off of any laser technical noise [10], and, depending on the input-pulse parameters, can lead to 50% temporal intensity fluctuations. While in some cases, empirical steps have been taken to reduce this noise, it is clear that a more complete understanding of its physical origin and scaling properties is essential if the supercontinuum is to be exploited to its full potential.

In this Letter, we show that the origin of this broadband noise is the nonlinear amplification of quantum fluctuations, both in the input laser light and in the Raman scattering process within the fiber. While this noise cannot be eliminated due to its fundamental origins, we identify methods of reducing its amplification through a judicious choice of input-pulse parameters. As well as their relevance to frequency metrology experiments, these results also represent a significant advance in the modeling of supercontinuum generation, as we present the first quantitative comparison between the measured noise on the supercontinuum and that predicted from stochastic numerical simulations.

Supercontinuum generation has been heavily investigated in bulk media since its observation in the 1960s [11]. Optical fiber is a particularly attractive medium due to long interaction lengths and potential telecommunication applications [12–14]. Supercontinua generated in conventional optical fiber have been very successfully described by the generalized nonlinear Schrödinger equation (NLSE) [11]. Recently, the NLSE has proven similarly successful in describing supercontinuum generated in microstructure fiber [15–18]. However, the NLSE is insufficient to describe the broadband amplitude noise; a stochastic NLSE [19] must be employed, which rigorously includes quantum-limited shot noise on the injected input field as well as spontaneous Raman fluctuations via a stochastic Langevin source term. Surprisingly, these small noise seeds are amplified into very large intensity fluctuations due to the inherent nonlinear processes involved in the supercontinuum generation. A similar noise amplification was observed in earlier work on continuum generation in more conventional optical fibers, and attributed to modulation instability on the pulse envelope induced by amplified spontaneous emission from the amplified input laser pulse [13,14].

The overall noise spectrum of the supercontinuum from the microstructure fiber actually has two components: the broadband component, discussed in this Letter, and a low-frequency component. The low-frequency component results from high sensitivity of the supercontinuum to initial input conditions [18,20,21], coupled with laser technical noise (i.e., laser power fluctuations or beam pointing instability), and can be reduced experimentally. In contrast, the broadband noise resulting from the input shot noise is fundamental to the supercontinuum generation process since the input shot noise and

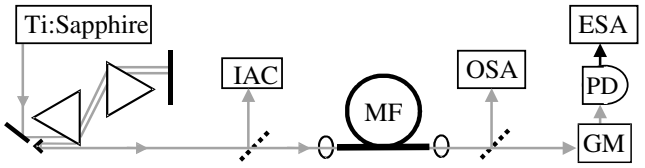

FIG. 1. Simplified schematic of the experimental setup. IAC, interferometric autocorrelator; MF, microstructure fiber; OSA, optical spectrum analyzer; GM, grating-based monochromator; PD, photodiode; ESA, electrical spectrum analyzer.

the spontaneous Raman scattering are quantum noise sources.

Figure 1 shows the experimental setup. An Ar^+ laser-pumped femtosecond Ti:sapphire laser provides pulses with a typical bandwidth of ~45 nm full width at half maximum (FWHM) centered at 810 nm at a 100 MHz repetition rate. A double-passed fused-silica prism pair introduces a linear chirp on the laser pulses, and interferometric autocorrelation measurements are used to infer both the input-pulse duration and chirp magnitude (in fs^2), assuming a $sech^2$ pulse intensity envelope. The chirped pulses with typical energies of 0.9 nJ are injected into a 15 cm long microstructure fiber with zero group-velocity dispersion at 770 nm [1], and the output is characterized using an optical spectrum analyzer and an apparatus dedicated to measuring the relative intensity noise (RIN). Here the supercontinuum is attenuated to prevent detector saturation, spectrally filtered by a monochromator with 8 nm bandwidth, and directed to either an infrared or a visible detector. The resulting electrical signal is fed into an electrical spectrum analyzer, where the rf noise power above the detector noise floor is measured. Typical raw data curves are shown in Fig. 2(a). The RIN in dBc/Hz [22] is obtained from this noise power, divided by the rf electrical bandwidth and the total detected power, and is measured at 10 nm increments across the supercontinuum. The noise power is measured at Fourier frequencies of 3 MHz and above, in order to avoid low-frequency Ti:sapphire laser noise [10]. Figure 2(b) reveals that the measured RIN is white noise, independent of Fourier frequency.

The experimentally measured spectral width and the noise are shown in Fig. 3. As noted by other groups, we see complicated spectral structure on the supercontinuum [15–18,20]. The RIN measurements also reveal for the first time the dramatic and complicated wavelength-dependent structure of the supercontinuum noise, where fluctuations as high as 20 dB are common. Under a wide variety of input-pulse conditions, the resulting supercontinua exhibit a consistent dip in the RIN at the input laser wavelengths ($\lambda_L \sim 810$ nm) and also across the Raman soliton on the infrared side of the spectrum ($\lambda_R \sim 1300$ nm). Otherwise, there is no universal correlation between the RIN and the optical spectrum.

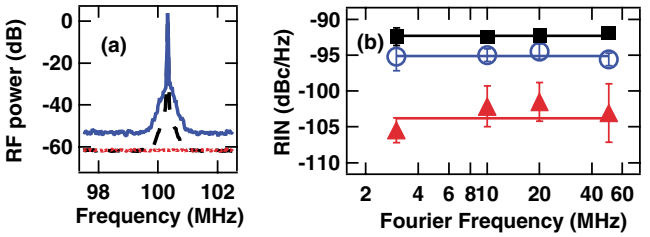

FIG. 2 (color online). (a) The rf power spectrum of the input laser (dashed line), a typical filtered supercontinuum (solid line), and the system noise floor (dotted line). (b) RIN as a function of Fourier frequency for three representative wavelengths: 620 nm (circles), 820 nm (triangles), and 920 nm (squares). The input pulse duration of 50 fs and pulse bandwidth of 45 nm corresponds to -290 fs^2 chirp.

The numerical simulations which model these measurements are based on the generalized NLSE [19,21]:

$$\frac{\partial E(z,t)}{\partial z} = i\sum_{k\geq 2}\frac{i^k\beta_k}{k!}\frac{\partial^k E}{\partial t^k} + i\gamma\left(1+\frac{i}{\omega_0}\frac{\partial}{\partial t}\right) \times\left[E(z,t)\left(\int_{-\infty}^{t} R(t')|E(z,t-t')|^2 dt' + i\Gamma_R(z,t)\right)\right].$$

Here $E(z,t)$ is the complex pulse envelope in a comoving frame and the β_k's (up to β_7) describe the fiber dispersion, which was calculated using the beam propagation method. The nonlinear coefficient $\gamma = 100\ W^{-1}\ km^{-1}$, based on a nonlinear index $n_2 = 2.6\times 10^{-20}\ m^2/W$ and an effective area of 2 μm^2. The response function $R(t) = (1-f_R)\delta(t) + f_R h_R(t)$ includes both instantaneous and delayed Raman contributions with the fractional Raman contribution $f_R = 0.18$. For h_R, we used the measured Raman response of silica. Spontaneous Raman noise appears as the multiplicative

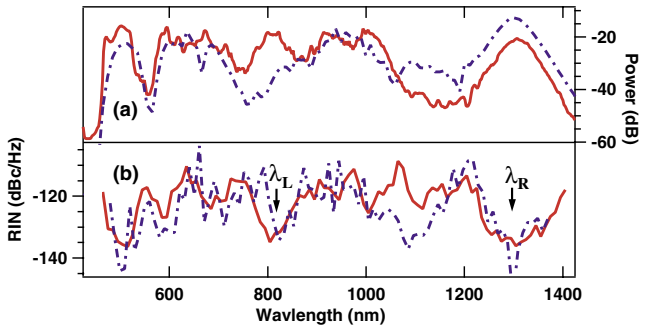

FIG. 3 (color online). (a) Spectrum and (b) total RIN as a function of wavelength across the supercontinuum for experiment (solid lines) and theory (dashed line) for an input pulse duration of 22 fs FWHM and a spectral bandwidth of 45 nm FWHM (i.e., with minimal chirp [23]) at an rf Fourier frequency of 3 MHz.

stochastic variable Γ_R, which has frequency domain correlations $\langle \Gamma_R(\Omega, z)\Gamma_R^*(\Omega', z')\rangle = (2f_R\hbar\omega_0/\gamma) \times |\mathrm{Im}[h_R(\Omega)]|[n_{\mathrm{th}}(|\Omega|) + U(-\Omega)]\delta(z - z')\delta(\Omega - \Omega')$ where the thermal Bose distribution $n_{\mathrm{th}}(\Omega) = [\exp(\hbar\Omega/k_BT) - 1]^{-1}$ and U is the Heaviside step function. The input-pulse initial conditions are those of the experimentally measured pulse duration and chirp, with the addition of quantum-limited shot noise. We stress that the magnitude of the quantum noise terms on the input pulse and due to spontaneous Raman scattering have no adjustable parameters. The RIN is calculated using an ensemble of 128 simulations with different random noise. The resulting supercontinua are assumed to be temporally separated by $(100\ \mathrm{MHz})^{-1}$ as in experiments to yield a time series of the intensity at each wavelength in the spectrum. The Fourier transform of this time series then gives the noise power spectrum, which is divided by the square of the average intensity to yield the RIN.

The dashed lines of Fig. 3 show numerical results for one set of simulations. Good qualitative agreement is observed between the experimental and simulated spectra and RIN. The simulations successfully reproduce the size of the fluctuations in RIN with wavelength, the average level of the RIN, and the decrease in RIN around the input laser and Raman soliton wavelengths.

The supercontinuum spectrum and noise level depend strongly on the input parameters of the laser pulse and many sets of data similar to those presented in Fig. 3 were taken under a variety of input conditions. The RIN always exhibits the complicated wavelength dependence shown in Fig. 3. However, in subsequent figures only the median RIN value is given, calculated across the supercontinuum. Nevertheless, it should be remembered that the deviations from this median value with wavelength are substantial. In fact, the statistics of the deviations are roughly consistent with Gaussian optical intensity fluctuations with unit fractional standard deviation. Because of averaging effects, both the experimentally measured and simulated RIN depend on the spectral bandwidth of the monochromator. Here the spectral bandwidth is 8 nm; reducing it to 1 nm increases the median RIN by ~3 dB.

Both the spectral width and the RIN increase with input-pulse energy, as shown in Fig. 4 for a moderately chirped input pulse. The experimental values are reproduced well in the simulation. Significantly, the spectral width increases with injected pulse energy at the expense of a corresponding increase in the noise. In fact, the linear increase in the RIN (in dBc/Hz) translates to an exponential increase in the associated fractional intensity fluctuations. Indeed, at the largest spectral width of ~600 nm, the relatively small RIN of −100 dBc/Hz corresponds to pulse-to-pulse fluctuations of ~7%.

Although the results above appear to suggest that the broadest supercontinuum spectral widths are necessarily associated with the largest RIN, additional experiments show that precise control of the input-pulse chirp permits

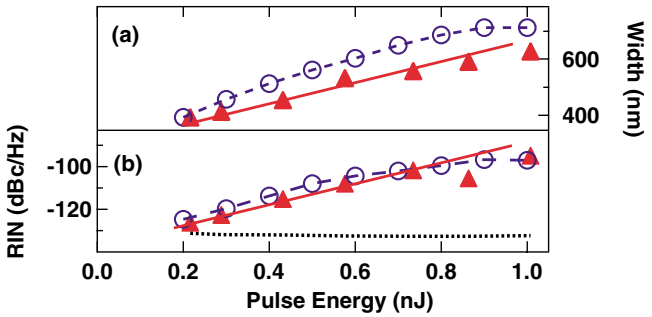

FIG. 4 (color online). (a) The −20 dB spectral width and (b) RIN on the supercontinuum as a function of the average power exiting the fiber for experiment (triangles) and theory (circles). Solid lines represent a linear fit to the experimental data. The dotted line is the contribution to the noise from the shot noise on the detected light. The input pulse duration of 47 fs and bandwidth of 42 nm corresponds to a chirp of $-280\ \mathrm{fs}^2$.

the generation of octave-spanning supercontinua with near detection shot-noise limited RIN. Figure 5 shows the supercontinuum spectral width and the median RIN as a function of input chirp [23]. As expected, large supercontinuum spectral widths are observed with the shortest (near transform-limited) input pulses, because shorter pulse duration at constant pulse energy implies higher peak power and thus enhanced nonlinear spectral broadening. In contrast, the median RIN, which depends strongly and asymmetrically on the pulse chirp, is smallest at the shortest pulse durations. At large negative chirps of $\sim -400\ \mathrm{fs}^2$, corresponding to pulse widths of ~60 fs, the RIN values can reach −83 dBc/Hz, corresponding to 50% fluctuations in the pulse-to-pulse amplitude. However, for pulses that are near transform limited or with a small positive chirp ($< +200\ \mathrm{fs}^2$), RIN values are only −130 dBc/Hz, which is just above

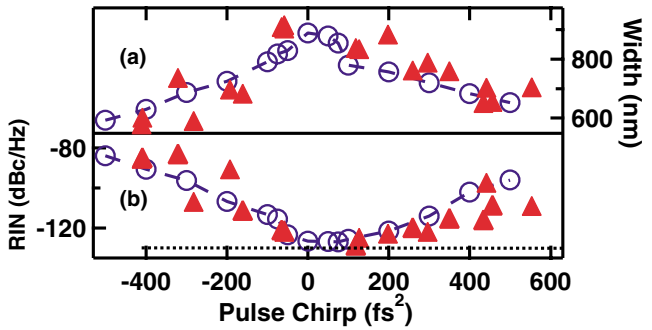

FIG. 5 (color online). (a) Supercontinuum −20 dB spectral width and (b) median RIN as a function of pulse chirp for experiment (triangles) and theory (circles). The dotted line is the detection shot noise contribution to the total RIN. A chirp variation of 0–650 fs^2 corresponds to a range of pulse widths from ~20 to 90 fs for a pulse bandwidth of 45 nm. The uncertainty in the experimental pulse chirp is about $\pm 30\ \mathrm{fs}^2$.

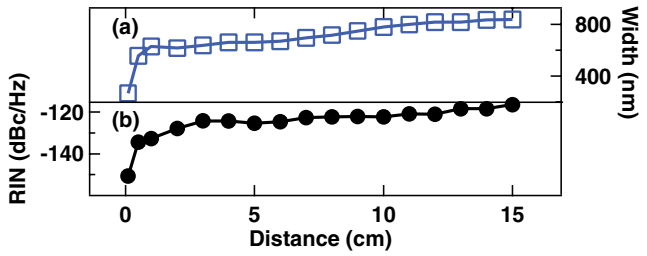

FIG. 6 (color online). Simulation results showing (a) −20 dB spectral width and (b) median RIN as a function of propagation distance in the fiber. The input pulse duration of 22 fs corresponds to second order dispersion of $-65\ \mathrm{fs}^2$ for a pulse bandwidth of 45 nm. The input energy is 0.85 nJ.

the detection shot-noise limit for our apparatus. Again, the measured dependence of RIN on chirp agrees well with the results of the simulation. Scatter in the data is attributed partly to uncertainty in the pulse chirp and energy. These data are taken with a laser spectral width of 45 nm; data taken at input spectral widths of 27 and 55 nm show similar dependencies.

While the noise above results from both input noise seeds, simulations show that the input shot noise is the dominant noise seed and that Raman scattering plays only a relatively minor role. When only Raman scattering noise is included numerically, the RIN is reduced by 20 dB; when only shot-noise is included, the RIN is reduced by less than ~1 dB. It is surprising that for an input shot noise of −172 dBc/Hz, the noise at the output can be as large as −80 dBc/Hz, corresponding to a nonlinear amplification of ~90 dB. In fact, there is a strong link between this nonlinear amplification and the initial spectral broadening, as shown in Fig. 6, where the simulated evolution of the spectral width and RIN is plotted as a function of propagation distance. The majority of the spectral broadening occurs in the first ~1 cm of propagation, which is also the distance scale on which the input shot noise is most strongly amplified. The strong dependence of the final RIN on the pulse chirp observed in Fig. 5 can also be understood in the context of Fig. 6. For short transform-limited pulses or pulses with a small positive chirp, which undergo initial compression, the spectral broadening is more rapid than for pulses with a large negative chirp. The more rapidly the spectrum broadens, the more rapidly the pulse will spread temporally through fiber dispersion, leading to a reduced overall noise amplification (akin to modulation instability gain), and therefore a reduced overall RIN.

In conclusion, we have experimentally characterized the broadband noise on supercontinua in microstructure fiber. Numerical simulations using the stochastic generalized NLSE show that this broadband noise results from the very basic noise processes of amplified input shot noise and Raman scattering. Thus, the supercontinuum output can exhibit excess noise approaching 50% amplitude fluctuations that arise directly from the shot noise on the input laser pulse. While the noise grows exponentially with input power, it is at a minimum for the shortest input-pulse duration, which is the same condition that yields the widest spectrum. These conditions bring the supercontinuum closer to the ideal realization of a broadband, phase-coherent source.

We thank Brian Washburn, Sarah Gilbert, and Leo Hollberg for valuable discussions.

[1] J. K. Ranka, R. S. Windeler, and A. J. Stentz, Opt. Lett. **25**, 25 (2000).
[2] T. A. Birks, W. J. Wadsworth, and P. S. J. Russell, Opt. Lett. **25**, 1415 (2000).
[3] I. Hartl *et al.*, Opt. Lett. **26**, 608 (2000).
[4] R. Holzwarth *et al.*, Appl. Phys. B **73**, 269 (2001).
[5] T. Udem, R. Holzwarth, and T.W. Hänsch, Nature (London) **416**, 233 (2002).
[6] S. A. Diddams *et al.*, Science **293**, 825 (2001).
[7] D. J. Jones *et al.*, Science **288**, 635 (2000).
[8] T. Udem *et al.*, in *Proceedings of The Hydrogen Atom: Precision Physics of Simple Atomic Systems*, edited by S. G. Karshenboim, F. S. Pavone, G. F. Bassani, M. Inguscio, and T.W. Hänsch (Springer-Verlag, Berlin, 2001), p. 125.
[9] L. Hollberg *et al.*, IEEE J. Quantum Electron. **37**, 1502 (2001).
[10] E. N. Ivanov, L. Hollberg, and S. A. Diddams, in *Proceedings of IEEE International Frequency Control Symposium, Crawley, WA, Australia, 2001* (IEEE, Piscataway, NJ, 2001), p. 117.
[11] R. R. Alfano, *The Supercontinuum Laser Source* (Springer-Verlag, New York, 1989).
[12] K. Mori, H. Takara, and S. Kawanishi, J. Opt. Soc. Am. B **18**, 1780 (2001), and references therein.
[13] H. Kubota, K. R. Tamura, and M. Nakazawa, J. Opt. Soc. Am. B **16**, 2223 (1999).
[14] O. Boyraz *et al.*, J. Lightwave Technol. **18**, 2167 (2000).
[15] A.V. Husakou and J. Herrmann, Phys. Rev. Lett. **87**, 203901 (2001).
[16] J. Herrmann *et al.*, Phys. Rev. Lett. **88**, 173901 (2002).
[17] B. R. Washburn, S. E. Ralph, and R. S. Windeler, Opt. Express **10**, 575 (2002).
[18] A. L. Gaeta, Opt. Lett. **27**, 924 (2002).
[19] P. D. Drummond and J. F. Corney, J. Opt. Soc. Am. B **18**, 139 (2001).
[20] X. Gu *et al.*, Opt. Lett. **27**, 1174 (2002).
[21] J. M. Dudley and S. Coen, Opt. Lett. **27**, 1180 (2002).
[22] dBc is defined as decibels referenced to the total dc power.
[23] A small ($\sim 500\ \mathrm{fs}^3$) third-order phase distortion is included, allowing the theory and experiment to agree on pulse duration at small chirp magnitudes.